Ferroelectrics, 339:191–199, 2006
Copyright © Taylor & Francis Group, LLC
ISSN: 0015-0193 print / 1563-5112 online
DOI: 10.1080/00150190600740150

Taylor & Francis
Taylor & Francis Group

Solid Solution Characterization of $Bi_4Ti_3O_{12}$ with Eu^{3+}

F. CAMACHO-ALANÍS,[1] M. E. VILLAFUERTE-CASTREJÓN,[1,*] G. GONZÁLEZ,[1] A. IBARRA-PALOS,[1] J. OCOTLÁN-FLORES,[2] R. Y. SATO-BERRÚ,[2] J. M. SANIGER,[2] M. VILLEGAS,[3] AND J. F. FERNÁNDEZ[3]

[1]Instituto de Investigaciones en Materiales, Universidad Nacional Autónoma de México, Ciudad Universitaria, A.P. 70-360, México D. F., México
[2]CCADET, Universidad Nacional Autónoma de México, Ciudad Universitaria, AP 70-188, México D. F., México
[3]Instituto de Cerámica y Vidrio, CSIC, Kelsen 5 Campus CSIC Cantoblanco, 28049 Madrid, España

$Bi_{4-x}Eu_xTi_3O_{12}$ solid solution was synthesized by coprecipitation and characterized by X-ray powder diffraction, thermal analyses, Raman spectroscopy and scanning electron microscopy. Sintering temperature influence on microstructure is discussed in base of the scanning electron microscopy micrographs. Differential scanning calorimetric curves show a reversible phase transition around 665° C with an intensity changes as a function of the Eu^{3+} doping content. The transformation enthalpy has a maximum value for the undoped $Bi_4Ti_3O_{12}$ samples and decreases with the increasing of Europium content. Finally, Raman studies of the samples show the vibrational changes induced by the Eu/Bi substitution.

Keywords Aurivillius structure; bismuth lead layered oxides; coprecipitation method; ferroelectric and piezoelectric materials

1. Introduction

In the last few years, there has been considerable interest in Bi-based layered oxides exhibiting ferroelectric, piezoelectric and other related properties due to their wide range of applications in technical devices. $Bi_4Ti_3O_{12}$ crystal structure consists on perovskite type units, $(Bi_2Ti_3O_{10})^{2-}$ and interleaved $(Bi_2O_2)^{2+}$ layers along the c-axis. In the $(Bi_2Ti_3O_{10})^{2-}$ units, Ti^{4+} ions are surrounded by oxygen octahedra, and Bi^{3+} ions occupy the outside of TiO_6 octahedra [1]. Bismuth Titanate (BiT) is currently one of the most technologically interesting materials because of its applications as ferroelectric memory [2]. Studies on the Bi substitution have been reported due to the enhancement of the ferroelectricity. The success property of lanthanum doping suggests further studies on the substitution of Bi by other rare earth ions [3]. Previous works have been done with BiT doped with Eu^{3+} [4],

Paper originally presented at IMF-11, Iguassu Falls, Brazil, September 5–9, 2005; received for publication January 26, 2006.
*Corresponding author. E-mail: mevc@servidor.unam.mx

but a complete study of the solid solution series including the solubility limit and thermal and spectroscopical characterization has not been performed up now. In the present paper $Bi_{4-x}Eu_xTi_3O_{12}$ (BiET) solid solution was prepared by coprecipitation and characterized by X-ray diffraction, thermal analysis studies and Raman spectroscopy.

2. Experimental

Samples were prepared by the coprecipitation method. Stoichiometric quantities of $Bi(NO_3)_35H_2O$ (Sigma-Aldrich 98%), Eu_2O_3 (Sigma-Aldrich 99.9%) dissolved in HNO_3 solution at 50% v/v and $Ti(OCH(CH_3)_2)_4$ (Aldrich 97%) dissolved in a HNO_3 and isopropanol (20/80) mixture were used as precursors. Powders were precipitated using an aqueous NH_4OH solution at 50% v/v. They were also filtered, washed with isopropanol until neutral pH was reached, dried at 80°C overnight and calcined at 950°C during 8 h.

X-ray powder diffraction (XRD) data were collected on a Bruker Instruments diffractometer D8 Advance, with Cu Kα radiation at 40 kV and 35 mA. For phase identification, the angle step and the counting time were 0.05° (2θ) and 1s respectively; the acquisition conditions for profile fitting were: step 0.02° (2θ) and counting time of 9 s.

Profile fitting including cell refinements, was carried out by using the Le Bail algorithm, in the pattern-matching mode with the Fullprof program [5].

Thermal analysis were carried out in a TGS-DSC simultaneous thermal analyzer (Nestzch, Jupiter STA 449C), with a flux on air of 60 ml/min with a heating rate of 10°C/min.

An Almega XR Dispersive Raman spectrometer equipped with an Olympus microscope (BX51) was used to obtain the Raman spectra. An Olympus ×10 objective (N.A. = 0.25) was used both for focusing the laser on the sample and collecting the scattered light in a 180° backscattering configuration. The scattered light was detected by a charge coupled device (CCD) detector, thermoelectrically cooling to −50°C. The spectrometer used a grating (2400 lines/mm) to resolve the scattered radiation and a notch filter to block the Rayleigh light. Raman spectra were accumulated over 25 s with a resolution of ∼4 cm^{-1}. The excitation source was 532 nm radiation from a Nd:YVO_4 laser (frequency-doubled) and the incident power at the sample was of ∼2 mW.

For SEM analysis, pellets were sinterized at different temperatures. In agreement to europium quantity, three thermal treatments were used, 850°C during 2 h, 1000°C during 2 h and 800°C during 1 h followed by 10 minutes at 1000°C and cooling again to 800°C, then the sample was retired from the furnace.

Samples were observed in a Scanning Electron Microscopy Leica Cambridge Stereo Scan 440 with an accelerating voltage of 20 kV and 500 pA of beam current in QBSD mode.

3. Results and Discussion

3.1. Analysis by X-ray Diffraction

X-ray powder diffraction patterns exhibit the characteristic Bragg reflections corresponding to the $Bi_4Ti_3O_{12}$ over the solid solution range $Bi_{4-x}Eu_xTi_3O_{12}$ ($0 \leq < x \leq 1.2$).

$Bi_4Ti_3O_{12}$ crystallizes in the monoclinic system [6], but when the amount of Eu^{3+} is increased, *a* and *b* parameters become similar, being practically equal in the solubility limit composition, x = 1.2, where a tetragonal distortion probably occurs. Figure 1 shows the increasing overlap of the (200) and (020) reflections for different Eu-Bi substitutions.

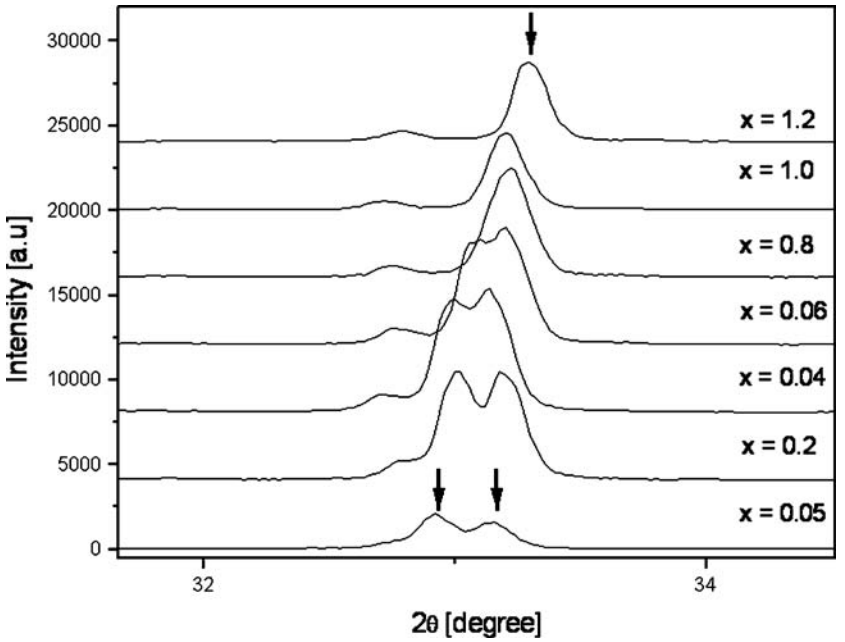

Figure 1. Overlapping behavior of (200) and (020) Bragg reflections in $Bi_{4-x}Eu_xTi_3O_{12}$.

Figure 2 is a plot of the unit cell parameters obtained from profile fitting analysis of the whole pattern as a function of the Eu^{3+} content. The substitution of Bi^{3+} results in a decrease of c as well as $a$and b parameters. The decrease of a is faster than b and they become very close for x values ≥ 0.8, resulting in the proposed tetragonal distortion.

3.2. TGA-DSC

It is well known that BiT has a ferroelectric transition at 675°C [7] which can be observed by differential scanning calorimetry as an exothermal peak. Figure 3 shows the exothermal peaks for the solid solution series $Bi_{4-x}Eu_xTi_3O_{12}$ from $x = 0$ to 0.8. The exothermal peak associated with the ferro-paraelectric transition is observed centered about 665°C for the BIT ($x = 0$). It is evident that the intensity of this peak decreases as Eu^{3+} content increases and for $x = 0.8$ the transition peak disappears. Together with the intensity decrease, a shift of the transition temperature toward lower values is also observed. This behavior is consistent with XRD results presented above where a and b unit cell parameters become closer when Eu^{3+} concentration increases. In the solid solution at $x = 0.8$, the initial ferro-paraelectric transition disappears due to the possible symmetry change from monoclinic to tetragonal. Under this assumption, the Bi/Eu substitution occurs as a solid solution with a solubility limit of $Eu = 1.2$, but originating an important structural distortion which results in a monoclinic-tetragonal transition before the solubility limit is reached.

3.3. Raman Spectroscopy

According with Wang, Kojima and Osada [3, 8, 9] the main $Bi_4Ti_3O_{12}$ vibrational modes are summarized in the Table 1.

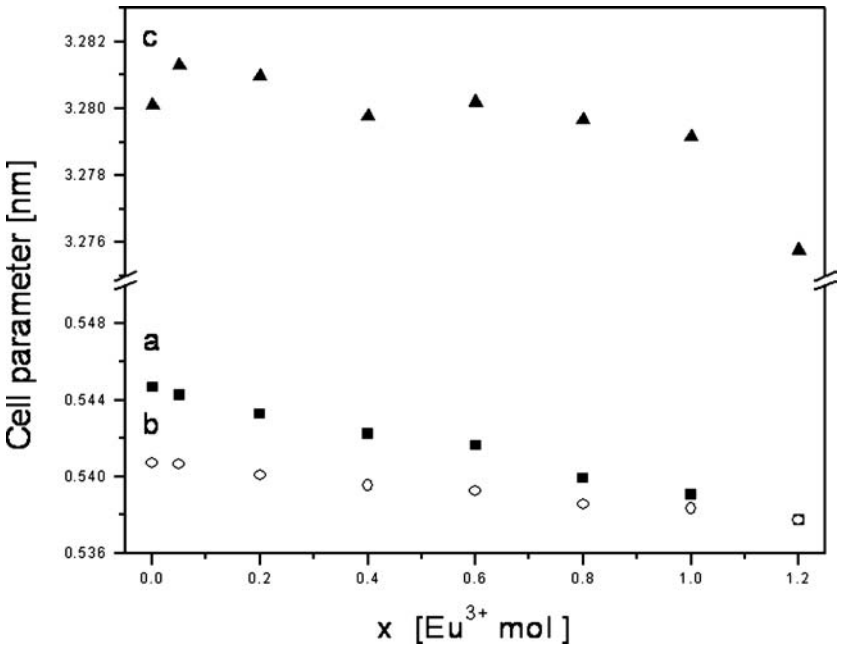

Figure 2. Variation of the unit cell parameters a, b and c versus x for the solid solution. $Bi_{4-x}Eu_xTi_3O_{12}$.

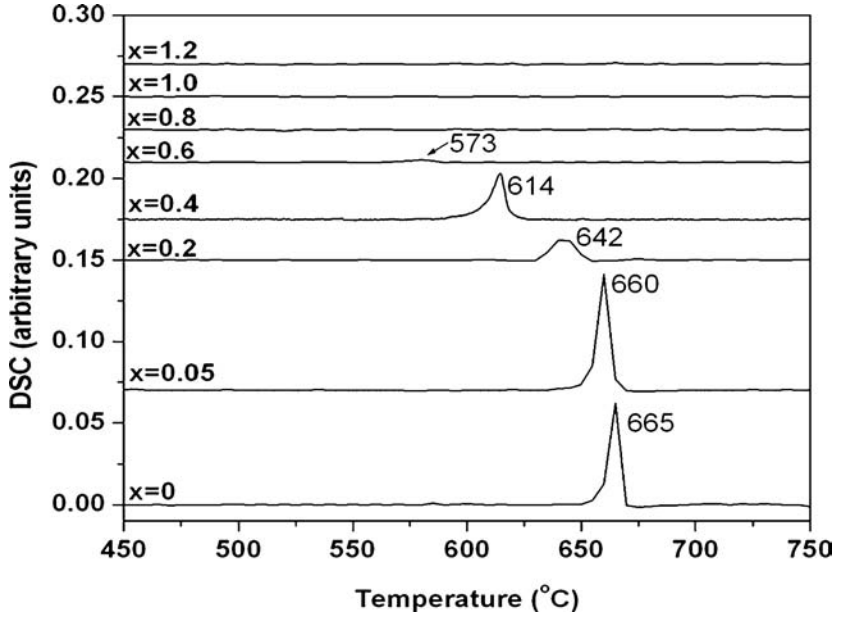

Figure 3. Exothermal peaks of $Bi_{4-x}Eu_xTi_3O_{12}$ for different x content.

Table 1
Mode frequencies of $Bi_4Ti_3O_{12}$ at room temperature

	ν (cm^{-1})
$(Bi_2O_2)^{2+}$ layer vibrational mode	60
Bi-O vibrational modes (perovskite site A)	96 and 119
Ti-O vibrational modes (TiO_6 octahedrons)	230, 268, 328, 563, 615 and 850

Figure 4 presents the Raman spectra of the $Bi_{4-x}Eu_xTi_3O_{12}$ series with different spectral region between 100 and 500 cm^{-1}. In this conditions the bands at 60 and 96 cm^{-1} assigned to the $(Bi_2O_2)^{2+}$ layer and one of the Bi-O vibrational modes of the perovskite site A can not be observed limiting the scope of the following discussion. Nevertheless, some interesting findings can be exposed. The band at 116 cm^{-1}, assigned to one of the Bi-O vibrational modes in the perovskite site A, remains almost unchanged until 0.4-0.6 Eu^{3+} concentration and disappears for Eu = 1.2 originating a new band at 159 cm^{-1}. Due to the experimental impossibility to observe the other Bi-O band vibrations a conclusive interpretation can not been done, but the trend observed at the 116 cm^{-1} band could suggest that the Eu/Bi substitution in the site A of the perovskite is evident only for x values equal or higher than 0.6.

Figure 5 shows the 100–1000 cm^{-1} Raman shift region, where the set of TiO_6 vibration modes are observed. A general comparison of the spectra of the solid solution series evidence strong changes in these bands, including the splitting of the one at (847 cm^{-1}), the disappearance of others (225 cm^{-1}) and significant intensity changes in all the cases. Knowing that Ti^{4+} at the octahedral sites cannot be substituted by Eu^{3+}, all these changes in the

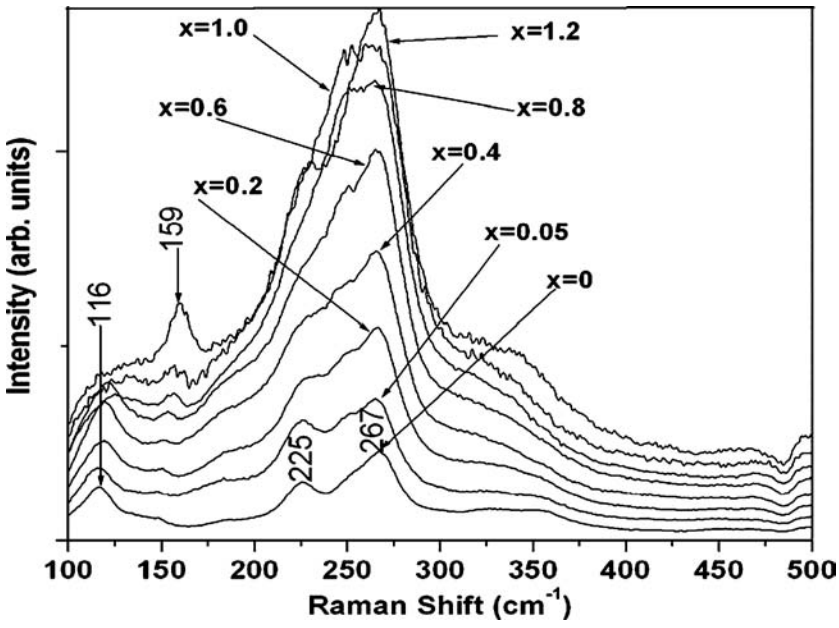

Figure 4. Raman spectra of $Bi_{4-x}Eu_xTi_3O_{12}$ from 100 to 500 cm^{-1}.

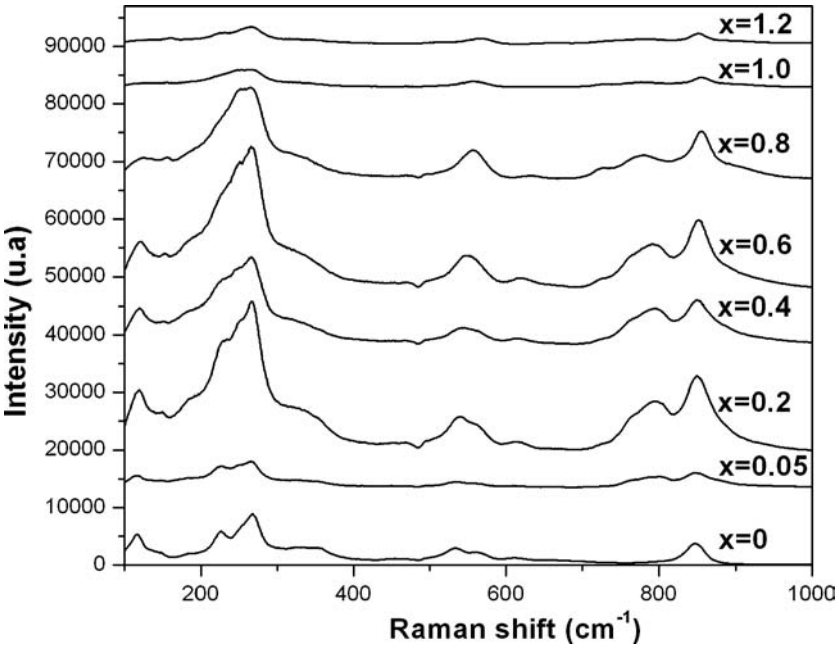

Figure 5. Raman spectra of $Bi_{4-x}Eu_xTi_3O_{12}$ for different concentration.

vibration modes of TiO_6 units must be related with the previously discussed structural distortion originated by the Eu/Bi substitution both in the $(Bi_2O_2)^{2+}$ layer and perovskite sites A (Table 1). The interesting changes observed in the Raman spectra deserve a more careful study in conjunction with other spectroscopic techniques and structural studies which are in progress.

3.4. Microstructure: SEM Images

We examine different microstructures of $Bi_{4-x}Eu_xTi_3O_{12}$ for compositions ranging from $x = 0$ up to $x = 1.2$. Depending on the Eu^{3+} content different features were observed, at 850°C during 2 h, only the samples with $x = 0$ and 0.05 present a high degree of densification and a platelet-like morphology with a grain size highly heterogeneous, as it shows in Fig. 6a.

At 1000°C during 2 h (Fig. 6b), the densification was achieved at Eu^{3+} contents ranging from $x = 0.2$ to $x = 0.8$. The grain size is considerable smaller ($\approx 2\ \mu$m) and more homogeneous than the BIT samples, with similar morphology. Samples with less Eu^{3+} content, melted and showed characteristics rounded grains.

In order to avoid the melt and to enhance the densification, we propose a thermal treatment at 800°C during 1 h followed by 10 minutes at 1000°C, followed by a rapid cooling ramp until 800°C; then samples were retired from the furnace to reach room temperature. The sinterized condition were determined for all the Eu^{3+} contents, the grain size evolutes and becomes small for Eu^{3+} content ranging from $x = 0.2$ up to $x = 0.8$ (around 5 microns), Fig. 6c shows the morphology of $Bi_{3.6}Eu_{0.4}Ti_3O_{12}$.

a)

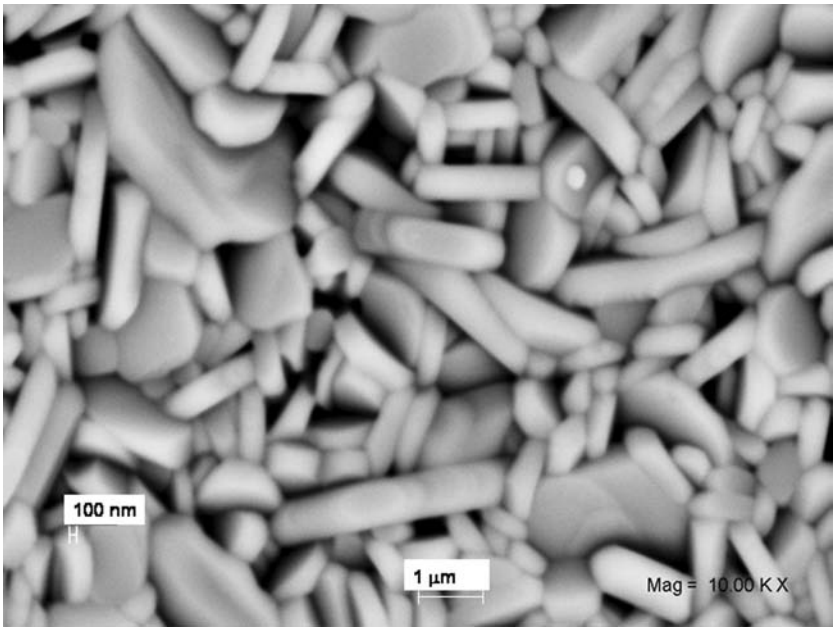

b)

Figure 6. Backscattered electron micrographs showing a platelet-like morphology of a) $Bi_4Ti_3O_{12}$ b) $Bi_{3.6}Eu_{0.4}Ti_3O_{12}$ c) $Bi_{3.2}Eu_{0.8}Ti_3O_{12}$. *(Continued)*

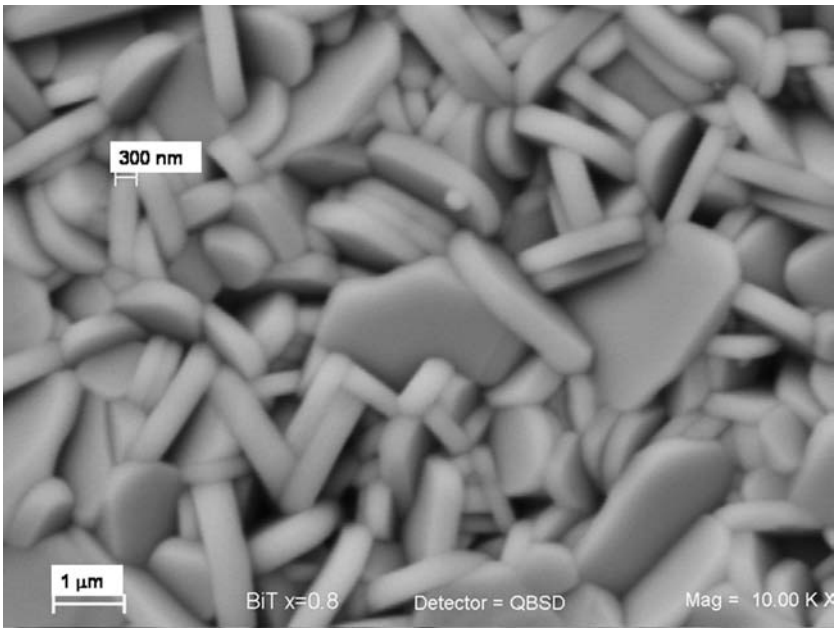

c)

Figure 6. (Continued)

4. Conclusions

The substitution of Bi by rare earth ions as the Eu^{3+}, presents interesting aspects from the structural point of view. In this study, we found a structural transition from a monoclinic to tetragonal cell depending on the Eu^{3+} amount, in our knowledge; this effect was unknown for Europium. The condition of densification and grain size strongly varies depending on the Eu^{3+} content. From the Raman studies, it seems to be reasonable to think that Eu/Bi substitution occurs both at the $(Bi_2O_2)^{2+}$ layers and perovskite site A, but further investigations should be done.

Acknowledgments

We thank for the financial support extended by DGAPA-UNAM PAPIIT No IN103603 and IN113814/15, CONACYT-SEP 2004-C01-47541 and CYTED PI.VIII-13 PROALERTA Project.

References

1. B. Aurivillius, Mixed bismuth oxides with layer lattices II. Structure of $Bi_4Ti_3O_{12}$. *Ark. Kemi*. **1**, 499–512 (1949).
2. K. Yong-Il, J. Min Ku, and W. Seong Ihl, Structural study of $Bi_4Ti_3O_{12}$ using neutron powder diffraction data. *J. Mat. Science Letters* **22**, 1655–1657 (2003).
3. Y. Wang, G. Xu, X. Zhang, Y. Feng, W. Tang, G. Cheng, and Y. Zhu, Structural and optical properties of $Bi_{4-x}Nd_xTi_3O_{12}$ thin films prepared by metal-organic solution deposition. *Materials Letters* **58**, 813–816 (2004).

4. K. T. Kim and C. I. Kim, $Bi_{3.25}Eu_{0.75}Ti_3O_{12}$ thin films with no polarization fatigue on prepared on Pt electrodes by using chemical solution routes. *J. Korean Phys. Soc*. **44**(1), 30–34 (2004).
5. J. Rodríguez-Carvajal, Fullprof: A program for Rietveld refinement and pattern matching analysis. Abstracts of the Satellite Meeting of the 15th Congress of the IUCr. Toulouse, France. (1990) 127.
6. D. Rae, J. G. Thompson, R. L. Withers, and A. C. Willis, Structure refinament of commensurately modulated Bismtuh Titanate, $Bi_4Ti_3O_{12}$. *Acta Cryst*. **B46**, 474–487 (1990).
7. E. C. Subbaro, Ferroelectricity in $Bi_4Ti_3O_{12}$ and its solid solutions. *Phys. Rev*. **122**, 804–807 (1960).
8. S. Kojima, R. Imaizumi, S. Hamazaki, and M. Takashige, Raman scattering study of bismuth layer-structure ferroelectrics. *Jpn. J. Appl. Phys*. **33**, 5559–5564 (1994).
9. M. Osada, M Tada, M. Kakihana, T. Watanabe, and H. Funakubo, Cation distribution and structural instability in $Bi_{4-x}La_xTi_3O_{12}$. *Jpn. J. Appl. Phys*. **40**, 5572–5575 (2001).

Copyright of Ferroelectrics is the property of Taylor & Francis Ltd and its content may not be copied or emailed to multiple sites or posted to a listserv without the copyright holder's express written permission. However, users may print, download, or email articles for individual use.